Abnormal B lymphocyte development and autoimmunity in hypoxia-inducible factor 1α-deficient chimeric mice

Hidefumi Kojima*†, Hua Gu*, Saeko Nomura*, Charles C. Caldwell*, Tetsuji Kobata†, Peter Carmeliet‡, Gregg L. Semenza§, and Michail V. Sitkovsky*¶

*Laboratory of Immunology, National Institute of Allergy and Infectious Diseases, National Institutes of Health, Bethesda, MD 20892-1892; †Division of Immunology, Institute for Medical Science, Dokkyo University School of Medicine, 880 Kitakobayashi, Mibu, Tochigi 321 0293, Japan; ‡Center for Transgene Technology and Gene Therapy, KU Leuven, Campus Gasthuisberg, Herestraat 49, B-3000 Leuven, Belgium; and §Institute of Genetic Medicine and Departments of Pediatrics and Medicine, The Johns Hopkins University School of Medicine, Baltimore, MD 21287-3914

Communicated by William E. Paul, National Institutes of Health, Bethesda, MD, December 28, 2001 (received for review October 19, 2001)

Immune cells are exposed to low oxygen tensions as they develop and migrate between blood and different tissues, but the mechanisms by which lymphocytes adapt to hypoxia are poorly understood. Studies reported here of hypoxia-inducible factor 1α (HIF-1α) in lymphocyte development and functions suggest that it has a critical role in regulation of these processes. HIF-1α deficiency in *Hif1*$\alpha^{-/-}$ → *Rag2*$^{-/-}$ chimeric mice results in dramatic and cell lineage-specific defects, which include appearance of abnormal peritoneal B-1-like lymphocytes, with high expression of B220 (CD45) receptor-associated protein tyrosine phosphatase and autoimmunity (accumulation of anti-dsDNA antibodies and rheumatoid factor in serum, deposits of IgG and IgM in kidney and proteinuria) as well as distortions of maturation of B-2 lymphocytes in bone marrow.

Immune cells are exposed to low oxygen tensions as they develop and migrate between blood and different tissues (1, 2), but the mechanisms by which lymphocytes adapt to hypoxia are poorly understood. Proliferating lymphocytes use ATP derived from glycolysis (3), and hypoxia-inducible factor 1 (HIF-1) mediates transcriptional activation of the genes encoding glucose transporters and glycolytic enzymes (4, 5), leading us to investigate the role of HIF-1 in lymphoid development. HIF-1 consists of a constitutively expressed HIF-1β subunit and a hypoxia and growth factor-induced HIF-1α subunit (4–7). HIF-1α-deficient (*Hif1*$\alpha^{-/-}$) mouse embryos die at midgestation (5, 8–10), which precludes analysis of later developmental events.

To test whether HIF-1α plays a role in the development and functioning of the mouse immune system *in vivo*, we used the RAG-2-deficient blastocyst complementation system (11), which allowed us to bypass embryonic lethality and analyze the effect of HIF-1α deficiency in T and B lymphocytes. The injection of pluripotent embryonic stem (ES) cells with a homozygous disruption of the gene encoding HIF-1α (*Hif1*$\alpha^{-/-}$) or wild-type (*Hif1*$\alpha^{+/+}$) ES cells with normal HIF-1α expression (12) into *Rag2*$^{-/-}$ C57BL/6 (B6) or normal B6 blastocysts resulted in the development of chimeric mice in which lymphocytes were derived from the injected ES cells. The analysis of these chimeric mice reported here revealed that deficiency in HIF-1α results in dramatic defects in development of B lymphocytes and in autoimmunity.

Materials and Methods

Mice. Mouse studies were performed in accordance with institutional guidelines of the National Institute of Allergy and Infectious Diseases, National Institutes of Health. Control wild-type mice and C57BL/6 (B6) mice, with or without RAG-2 deficiency as a source of blastocysts, were purchased from Taconic Farms and maintained at the National Institutes of Health animal facility. Chimeric mice were obtained by injecting ES cells into blastocysts of B6 background *Rag2*$^{-/-}$ or *Rag2*$^{+/+}$ wild-type mice as described (11). ES cells with homozygous disruption of HIF-1α genes were generated as previously described (12).

Flow Cytometry. Single-cell suspensions were prepared, and cells were stained with fluorescein isothiocyanate (FITC), phycoerythrin, CyChrome, and allophycocianin-labeled Ab or in combination with biotinylated Ab and dye-conjugated streptavidin (PharMingen) followed by analysis of duplicates or triplicates on a FACScalibur by using CELLQUEST software (Becton Dickinson). All mAbs used for flow cytometry in this study were purchased from PharMingen.

Antibody Titration. Total serum IgM and IgG were measured by using Mouse Ig ELISA quantitation kits (Bethyl Laboratories, Montgomery, TX) and ELISA starter accessory package (Bethyl Laboratories) according to manufacturer's instructions. The titers of anti-dsDNA Ab in mouse serum were determined by using 0.001% of protamine sulfate (Sigma) and the calf thymus DNA (Sigma) coated ELISA plates. Horseradish peroxidase-conjugated goat anti-mouse IgM (Caltag, South San Francisco, CA) and goat anti-mouse IgG (ICN) were used for detection of anti-dsDNA IgM and IgG, respectively. The titers of rheumatoid factors (RF) in serum were analyzed by using goat IgG precoated ELISA plates. IgM-RF and IgG-RF were detected by using horseradish peroxidase-conjugated anti-mouse IgM and anti-mouse IgG, respectively. The titers of anti-dsDNA Ab and RF are determined as absorbance at 450 nm wavelength.

Immunohistochemistry. The visualization of IgM and IgG on paraffin-embedded sections of kidney was performed by using biotin-labeled anti-IgM and anti-IgG mAb and fuchsia-conjugated streptavidin reagents (Dako).

Measurement of Protein Levels in Urine. The protein concentration in urine samples from mice was determined by using a Microprotein kit (Sigma).

Results

The HIF-1α-deficient chimeric mice had short limbs (data not shown) and were found to have ES cell-derived lymphocytes as defined by the Ly-9.1 allelic marker. Analysis of the gated Ly-9.1$^+$ cells from *Hif1*$\alpha^{-/-}$ → *Rag2*$^{+/+}$ B6 chimeras revealed the presence of rather normal HIF-1α-deficient CD4$^+$ and CD8$^+$ T

Abbreviations: HIF-1, hypoxia-inducible factor 1; RAG-2, recombination activating gene 2; ES, embryonic stem; RF, rheumatoid factors.

¶To whom reprint requests should be addressed. E-mail: mvsitkov@helix.nih.gov.

The publication costs of this article were defrayed in part by page charge payment. This article must therefore be hereby marked "*advertisement*" in accordance with 18 U.S.C. §1734 solely to indicate this fact.

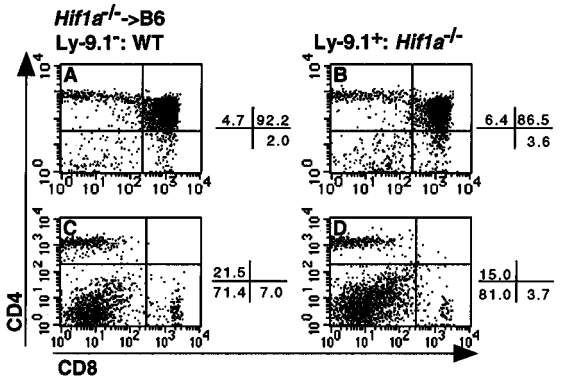

Fig. 1. Flow cytometry analysis of *Hif1a*$^{-/-}$ T cell development. Thymocytes (*A* and *B*) and spleen cells (*C* and *D*) from *Hif1a*$^{-/-}$ → *Rag2*$^{+/+}$ normal B6 chimera (4 weeks old) were stained with anti-Ly-9.1 mAb, anti-CD4-mAb, and anti-CD8 mAb. Stained cells were gated to enable characterization of *HIF-1α*$^{+/+}$ blastocyst-derived Ly-9.1 negative fraction (*A* and *C*) and *Hif1a*$^{-/-}$ ES-derived Ly-9.1 positive fraction (*B* and *D*) by studies of the expression of CD4 and CD8.

cell subsets in the thymus (Fig. 1 *A* and *B*), spleen (Fig. 1 *C* and *D*), lymph nodes and peripheral blood of chimeric mice (data not shown), and dramatic distortions in phenotype of B cells (Fig. 2; see also Figs. 4 and 5).

Studies of defects in bone structure are in progress, but in the first series of experiments, we focused on investigations of changes in well described surface markers of B lymphocytes (13–17). Analysis of peritoneal lymphocytes in *Hif1α*$^{-/-}$ → *Rag2*$^{-/-}$ chimeric mice revealed dramatic changes in expression of B1 cell-defining CD5 and B220 surface markers (Fig. 2), whereas no differences were found in levels of expression of CD5 and B220 between control *Hif1α*$^{+/+}$ ES → *Rag2*$^{-/-}$ chimeric mice and normal B6 or 129 mice (data not shown). The CD5^{dull}B220$^{-/dull}$ subset that was observed in *Hif1α*$^{+/+}$ chimeras (Fig. 2*A*) was lost, whereas accumulation of unusual CD5^{+}/B220^{+} cells was detected in *Hif1α*$^{-/-}$ chimeras (Fig. 2*B*). The CD5^{+} IgM^{high}/IgD$^{low\text{-}inter}$ expression pattern of these B220^{+}cells in *Hif1α*$^{-/-}$ chimeras (Fig. 2 *C–H*) is similar to peritoneal B1 cells (15), but the CD5^{+} cells in *Hif1α*$^{-/-}$ chimeras had much higher levels of B220 expression, leading us to designate these unusual

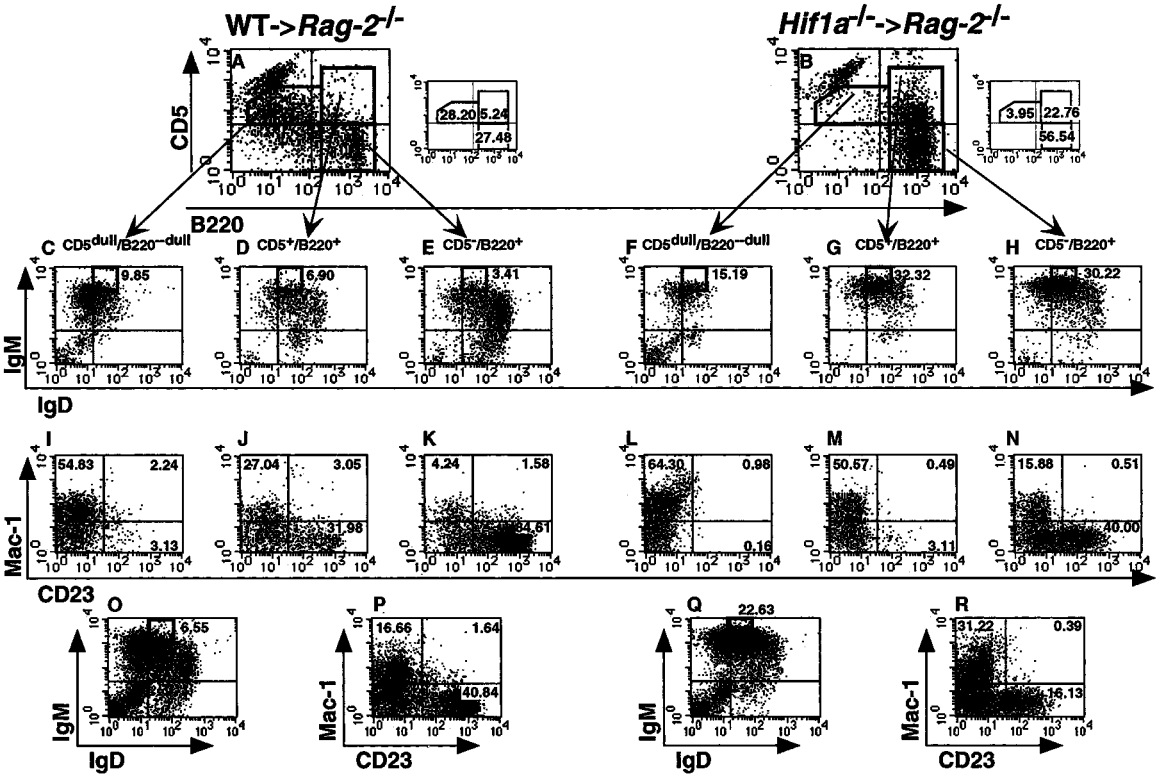

Fig. 2. Flow cytometry analysis of *Hif1a*$^{-/-}$ B cell development. Flow cytometry analysis reveals abnormal B-1-like lymphocytes in the peritoneal cavity of *Hif1a*$^{-/-}$ → *Rag2*$^{-/-}$ chimeric mice. Panels depict representative flow cytometric experiments comparing cells from age-matched *Hif1a*$^{-/-}$ (*B*, *F–H*, *L–N*, *Q*, and *R*) and *Hif1a*$^{+/+}$ chimeric mice (*A*, *C–E*, and *O*) or with age-matched wild-type 129 mice (*I–K* and *P*). Cells were gated according to forward vs. side scatter, and then ES cell-derived Ly-9.1^{+} cells were gated to be further analyzed for staining with mAb to various surface markers (13–17). Single-cell suspensions of peritoneal cavity cells were stained and analyzed by flow cytometry. The assays were done in triplicates or duplicates. The results are representative outcomes from studies of three generations of independently derived chimeric mice. Peritoneal cavity cells of control wild-type (WT *Hif1a*$^{+/+}$ ES → *RAG-2*$^{-/-}$) chimera (*A*) and from *Hif1a*$^{-/-}$ ES → *RAG-2*$^{-/-}$ chimera (*B*) were harvested and stained with anti-Ly-9.1 mAb, anti-CD5 mAb, and anti-B220 mAb. Then, ES-derived Ly-9.1^{+} cells were analyzed for expression of both CD5 and B220 by flow cytometry. This was followed by analysis of different CD5/B220-defined cell populations for expression of such B-1 cell markers like IgM vs. IgD (*C–H*, *O*, and *Q*) and Mac-1 vs. CD23 (*I–N*, *P*, and *R*). Demonstration of typical IgM^{high} and IgD^{low} peritoneal B-1 and B-1-like cells in wild-type (WT) and HIF-1α-deficient chimeras was accomplished by gating for analysis B220$^{negative\text{-}dull}$/CD5^{dull} fraction (*C* and *F*), B220^{+}/CD5^{+} fraction (*D* and *G*), and B220^{+}/CD5^{-} fraction (*E* and *H*). IgM/IgD expression on total peritoneal cavity cells are depicted in *O* (WT chimera) and in *Q* (*Hif1a*$^{-/-}$ → *RAG-2*$^{-/-}$ chimera). Proportions of cells are indicated in each panel. The presence of typical B1 cells among B220$^{negative\text{-}dull}$/CD5^{dull} fraction of peritoneal cells from WT mouse and among B220^{+}/CD5^{+} fraction of *Hif1a* chimeras was confirmed in studies of Mac-1 (CD11b) vs. CD23 expression on peritoneal cells collected from 129 mouse (*I–K*) and from *Hif1a*$^{-/-}$ → *RAG-2*$^{-/-}$ chimera (*L–N*). In this experiment, cells were analyzed for the expression levels of Mac-1 and CD23 after cells were stained with anti-CD5 mAb, anti-B220 mAb, anti-Mac-1 mAb, and anti-CD23 mAb. B220$^{negative\text{-}dull}$CD5^{dull} fraction (*I* and *L*), B220^{+}/CD5^{+} fraction (*J* and *M*), and B220^{+}/CD5^{-} fraction (*K* and *N*) were gated for analysis. Expression of Mac-1 and CD23 on total peritoneal cavity cells is depicted in *P* (WT mouse) and in *R* (*Hif1a*$^{-/-}$ → *RAG-2*$^{-/-}$ chimera). It was confirmed in control experiments that profiles of CD5/B220 expression on Ly-9.1^{+} cells and Ly-9.1^{+}/Ly-9.1^{-} cells in *Hif1a*$^{-/-}$ ES → *RAG-2*$^{-/-}$ chimera were similar. This allowed the comparison of cells in *C–R* without gating for Ly-9.1 expression.

cells as B-1-like. In addition, $CD5^{-}B220^{+}$ cells in the peritoneum of *Hif1α*$^{-/-}$ chimeras had significantly increased IgM^{high}/IgD^{low} populations (from 3.41% in control to 30.22%, Fig. 2 *E* and *H*). The same was true in studies of $CD5^{+}B220^{+}$ cells, which were found to have an increased proportion of IgM^{high}/IgD^{low} cells (from 6.9% to 32.32%, Fig. 2 *D* and *G*). The increase in proportion and number of cells with B-1 phenotype ($Mac\text{-}1^{+}/CD23^{-}$) in *Hif1α*$^{-/-}$ chimeras was further confirmed in studies of peritoneal $CD5^{+}B220^{+}$ (Fig. 2 *J* and *M*) and of $CD5^{-}B220^{+}$ B-1 cells (Fig. 2 *K* and *N*). The increase in cells with abnormal B-1 phenotype was accompanied by a corresponding decrease in proportions of other cells (e.g. $Mac\text{-}1^{-}/CD23^{+}$, from 84% to 40%) in the peritoneum of *Hif1α*$^{-/-}$ mice (Fig. 2 *K* and *N*). Thus, whereas the total numbers of cells harvested from the peritoneum of control and HIF-1α-deficient mice are similar (data not shown), the proportion of IgM^{high}/IgD^{low} (Fig. 2 *O* and *Q*) and $Mac\text{-}1^{+}/CD23^{-}$ (Fig. 2 *P* and *R*) cells with B-1 phenotype is much larger in *Hif1α*$^{-/-}$ chimeras.

B-1 cells were reported to play a role in autoimmunity (16), and this prompted us to investigate the possibility of autoimmunity in *Hif1α*$^{-/-}$ chimeras with abnormal B-1-like cells. Subsequent studies of 6–8-week-old mice revealed markedly increased levels of both IgM and IgG anti-dsDNA autoantibodies (Fig. 3 *C* and *D*) in the serum of the *Hif1α*$^{-/-}$ chimeras. Total IgM levels were also increased in the serum of *Hif1α*$^{-/-}$ chimeras, whereas no difference in IgG levels was found (Fig. 3 *A* and *B*). This was accompanied by extensive deposits of IgM and IgG in kidneys of *Hif1α*$^{-/-}$, but not *Hif1α*$^{+/+}$, chimeras (Fig. 3 *E–H*). Evidence of autoimmune disease was also provided by the demonstration of proteinuria (Fig. 3*I*) and accumulation of RF (Fig. 3 *J–L*) in *Hif1α*$^{-/-}$ chimeras. Taken together, these observations suggest that HIF-1α is important for proper regulation of B1 cell homeostasis and that HIF-1α deficiency results in autoimmunity.

Deficiency in HIF-1α also results in age-dependent defects in the subset composition of immature and mature conventional B-lymphocytes (B-2 cells) in bone marrow as reflected by the absence of IgM^{high} and $B220^{high}$ (immature) population after 8 weeks of age (Fig. 4 *D–G*) and appearance of $B220^{high}$ cells after 12 weeks (Fig. 4 *H–K*).

Studies of B-2 cells allowed us to discriminate between cell-autonomous and noncell autonomous effects of HIF-1α deficiency [e.g., because of the defects in HIF-1α-dependent angiogenesis and organogenesis (4, 7, 8) in *Hif1α*$^{-/-}$ chimeric mice] by analysis of conventional B-2 cells in *Hif1α*$^{-/-}$ → *Rag2*$^{+/+}$ WT B6 chimeras, in which development of *Hif1α*$^{-/-}$ B-2 cells could be compared with *Hif1α*$^{+/+}$ B-2 cells within the same individual chimeric mice (Fig. 4*A*). The normal maturation of Ly-9.1^{-} *Hif1α*$^{+/+}$ B-2 lymphocytes of B6 blastocyst origin (Fig. 4*B*) and the block of maturation of Ly-9.1^{+} *Hif1α*$^{-/-}$ B-2 lymphocytes of ES origin (Fig. 4*C*) were observed in *Hif1α*$^{-/-}$ → *Rag2*$^{+/+}$ B6 chimeras (4 weeks old), suggesting that effects of HIF-1α deficiency on B cell development are cell-autonomous.

Further analysis of bone marrow B cell development in *Hif1α*$^{-/-}$ → *Rag2*$^{-/-}$ chimeras by using the B cell differentiation marker HSA revealed a decrease from 46.36% to 8.24% among HSA^{high} $B220^{+}$ B cell progenitors and a dramatic increase in immature HSA^{-} $B220^{-}$ bone marrow cells in *Hif1α*$^{-/-}$ → *Rag2*$^{-/-}$ chimeras (Fig. 5*A*). The decrease in HSA^{high} $CD43^{-}B220^{+}$ B cell progenitors (Fig. 5*B*) and results of IgM vs. B220 and CD43 vs. B220 analysis (Fig. 4) suggest that HIF-1α may be required for the transition from large preB to small preB [fraction D by Hardy *et al.* (17)] to immature B (fraction E) cells.

Further studies revealed that HIF-1α deficiency results in the depletion of highly proliferating cells among B cell progenitors in bone marrow, as $CD43^{-}$ $B220^{+}$ HSA^{high} cells, which are almost completely lost in *Hif1α*$^{-/-}$ → *Rag2*$^{-/-}$ chimeras (Fig. 5*B*), are the most highly proliferating subset based on expression

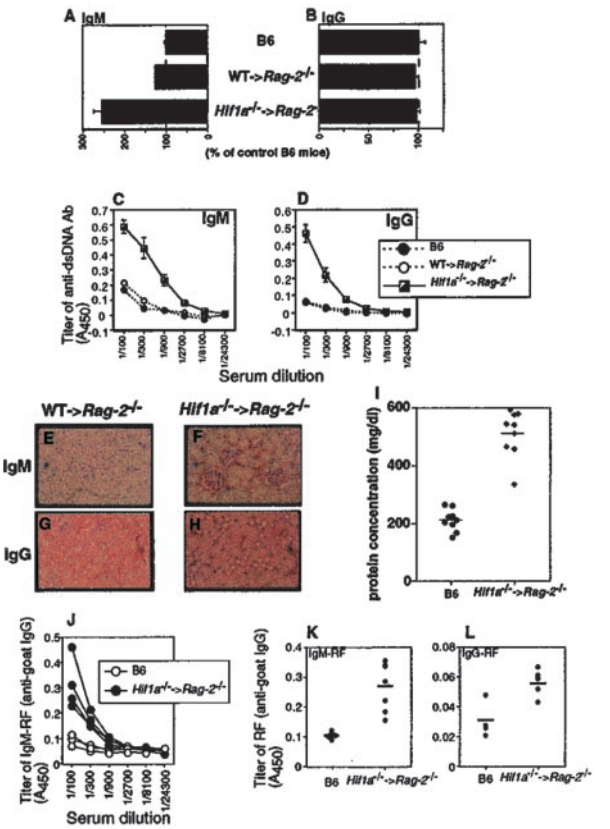

Fig. 3. Demonstration of autoimmunity in Hifla$^{-/-}$ >Rag-2$^{-/-}$ chimeras. (*A* and *B*) Determination of concentrations of total IgM and IgG in serum of *Hif1a*$^{+/+}$ *(WT)* → *Rag2*$^{-/-}$ and *Hif1a*$^{-/-}$ → *Rag2*$^{-/-}$ chimeric mice. Results of measurements of serum IgM and IgG are presented as % of serum IgM and IgG levels, respectively, in control B6 mice. Mouse Ig ELISA quantitation kits (Bethyl Laboratories) and ELISA starter accessory package (Bethyl Laboratories) were used to measure serum Ab titer according to manufacturer's instructions. (*C* and *D*) Demonstration of increased concentration of anti-dsDNA IgM and IgG auto Ab in serum of *Hif1a*$^{-/-}$ → *Rag2*$^{-/-}$ vs. *Hif1a*$^{+/+}$ → *Rag2*$^{-/-}$ chimeric mice and normal B6 mice. Serum samples were diluted as indicated, and concentration of anti-dsDNA Abs was tested by ELISA. The titer of anti-dsDNA Ab in mouse serum was determined by using 0.001% of protamine sulfate (Sigma) coated ELISA plates. The calf thymus DNA (Sigma) and horseradish peroxidase-conjugated goat anti-mouse IgM (Caltag) and goat anti-mouse IgG (ICN) were used for detection of anti-dsDNA IgM and IgG. The anti-dsDNA Ab titers are presented in relative units as absorbance at 450 nm wavelength. (*E–H*) The immunohistochemical localization of IgM and IgG deposits of paraffin-embedded sections of kidney from *Hif1a*$^{-/-}$ → *Rag2*$^{-/-}$ chimeras (*F* and *H*) and WT controls (*E* and *G*). Fuchsia-colored staining indicates location of IgG or IgM. The visualization of IgM and IgG on paraffin-embedded sections of kidney from *Hif1a*$^{-/-}$ → *Rag2*$^{-/-}$ chimeras and WT → *Rag2*$^{-/-}$ controls was performed by using anti-IgM and anti-IgG mAb and labeled streptavidin biotin reagents (Dako). (*I*) Increased levels of proteins in urine from *Hif1a*$^{-/-}$ → *Rag2*$^{-/-}$ chimeras. The protein concentration in urine samples from eight age-matched *Hif1a*$^{-/-}$ → *Rag2*$^{-/-}$ chimeras and control B6 mice was determined by using the Microprotein kit (Sigma). (*J–L*) Demonstration of increased concentration of RF in serum of *Hif1a*$^{-/-}$ → *Rag2*$^{-/-}$ chimeric mice as compared with normal B6 mice. The titers of rheumatoid factors in serum were determined by using goat IgG precoated ELISA plates. IgM-RF and IgG-RF were detected by using horseradish peroxidase-conjugated anti-mouse IgM and anti-mouse IgG, respectively. Serum samples were diluted as indicated and were tested (*J*). Serum samples diluted 100 times were used to compare levels of RF-IgM and RF-IgG in serum samples from seven *Hif1a*$^{-/-}$ → *Rag2*$^{-/-}$ chimeras and six B6 mice (*K* and *L*). Six- to eight-week-old mice were used in these series of experiments.

of a nuclear cell proliferation-associated antigen Ki-67 (18) on cells from 129 mice (Fig. 5*C*). Indeed, expression of Ki-67 on *Hif1α*$^{-/-}$ $CD43^{-}B220^{+}$ bone marrow cells was much less than on

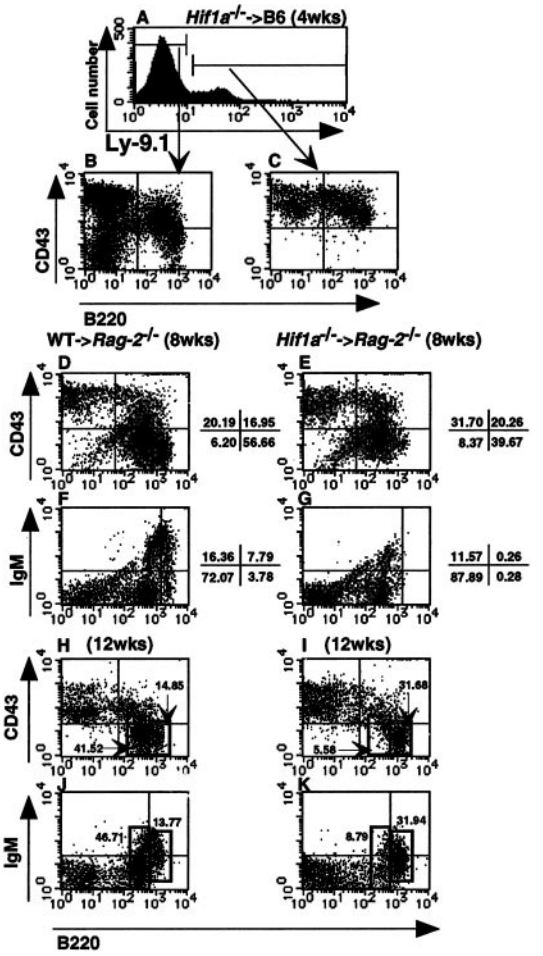

Fig. 4. Cell-autonomous effects of the HIF-1α deficiency and the characterization of age-dependent defects in B cell development in bone marrow of HIF-1α-deficient chimeras. (*A–C*) The presence of normal HIF-1$\alpha^{+/+}$ B cells and their progenitors and the absence of HIF-1$\alpha^{-/-}$ B cell subsets within the bone marrow of the same chimeric animal. Bone marrow cells from *Hif1a*$^{-/-}$ → *Rag2*$^{+/+}$ normal B6 chimera (4 weeks old) were stained with anti-Ly-9.1 mAb (*A*) and anti-CD43-mAb and anti-B220 mAb (*B* and *C*). Stained cells were gated to enable characterization of HIF-1$\alpha^{+/+}$ blastocyst-derived Ly-9.1 negative fraction (*B*) and *Hif1a*$^{-/-}$ ES-derived Ly-9.1 positive fraction (*C*) by studies of the expression of B cell maturation markers CD43 and B220. (*D–K*) Distortion and age-dependent changes in B cell subset composition in bone marrow of *Hif1a*$^{-/-}$ → *Rag2*$^{-/-}$ chimeras. Bone marrow cells from both WT → *Rag2*$^{-/-}$ chimera (*D*, *F*, *H*, and *J*) and *Hif1a*$^{-/-}$ → *Rag2*$^{-/-}$ chimera (8 weeks old and 12 weeks old) (*E*, *G*, *I*, and *K*) were stained with anti-Ly-9.1 mAb, and Ly-9.1-positive cells were gated and analyzed for expression of CD43 vs. B220 or IgM vs. B220 (*F*, *G*, *J*, and *K*). Proportions of cells in designated areas of graphs are indicated.

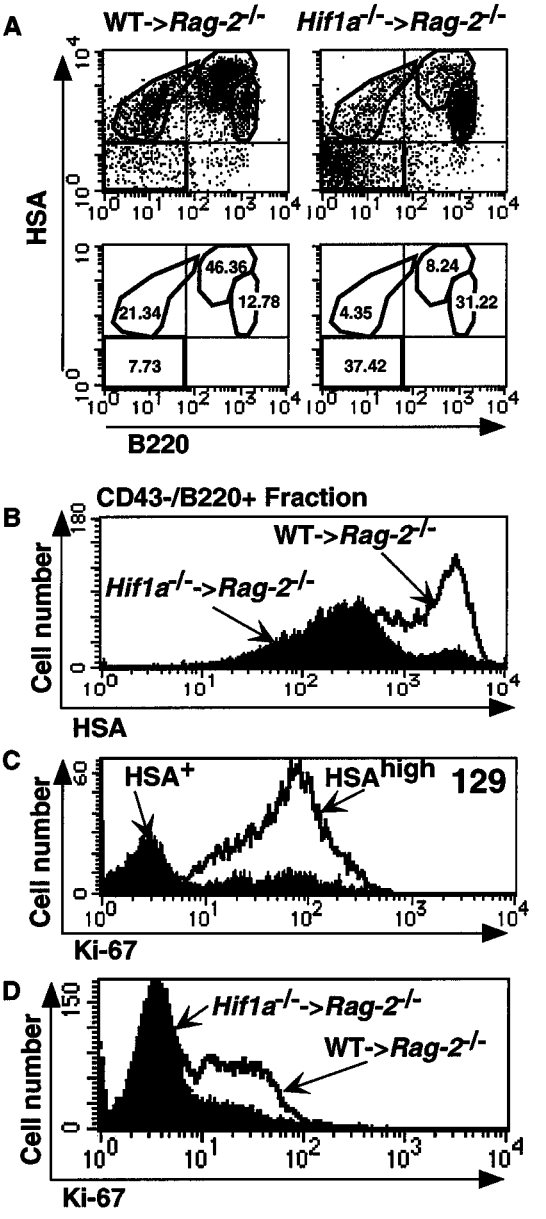

Fig. 5. Defects in subset distribution and proliferation of *Hif1a*$^{-/-}$ bone marrow B cells in HIF-1α-deficient chimeras. Bone marrow cells harvested from *Hif1a*$^{-/-}$ → *Rag2*$^{-/-}$ chimeras and control 129 mice or WT → *Rag2*$^{-/-}$ chimeras were stained with anti-Ly-9.1 mAb to identify ES cell origin B cell progenitors, which were then analyzed for the expression of B cell differentiation markers CD43, B220, and HSA as well as for the expression of nuclear proliferation marker Ki-67. (*A*) Expression of HSA and B220 among Ly.9.1^{+} cells from 12-week-old *Hif1a*$^{-/-}$ → *Rag2*$^{-/-}$ and WT → *Rag2*$^{-/-}$ chimeras. Proportions of cells in designated areas of graphs are indicated. (*B*) The decrease in HSA expressing cells among CD43^{-}B220^{+} preB cells. Expression levels of HSA among CD43^{-}B220^{+} bone marrow cells were evaluated after gating cells, which were stained with anti-Ly 9.1 mAb, anti-CD43 mAb, anti-B220 mAb, and anti-HSA mAb. (*C*) Highly proliferating cells are found among CD43^{-}B220^{+} HSA^{high} B cell progenitors in bone marrow of control *Hif1a*$^{+/+}$ normal 129 mice as detected by the expression of cell proliferation marker Ki-67. Bone marrow cells from normal 129 mouse were stained with anti-CD43-mAb, anti-B220 mAb, anti-HSA mAb, and anti-Ki-67-mAb. CD43^{-}/B220^{+} bone marrow cells were further gated into HSA^{high} and HSA^{+} cell fractions, and expression levels of Ki-67 were determined in each cell fraction. (*D*) Decreased Ki-67 expression among CD43^{-}/B220^{+} bone marrow cells from *Hif1a*$^{-/-}$ → *Rag2*$^{-/-}$ chimeras. Bone marrow cells from *Hif1a*$^{-/-}$ → *Rag2*$^{-/-}$ chimeras and WT → *Rag2*$^{-/-}$ chimeras were stained with anti-Ly9.1 mAb, anti-CD43-mAb, anti-B220 mAb, and anti-Ki-67-mAb. Then, Ly9.1^{+} bone marrow cells were further gated into CD43^{-}B220^{+} cell fractions to compare expression levels of Ki-67.

CD43^{-}B220^{+} cells from *Hif1*$\alpha^{+/+}$ WT → *Rag2*$^{-/-}$ chimeras (Fig. 5*D*).

Discussion

The multiple roles of hypoxia-inducible HIF-1α in cell metabolism and functions (4–10) and the predominance of hypoxic conditions in lymphoid tissues *in vivo* (2) suggested that this protein could be involved in the development and regulation of cells of the immune system. The direct testing of the possible role of HIF-1α in the immune system was precluded by midgestation death of HIF-1α-deficient (*Hif1*$\alpha^{-/-}$) mouse embryos (5, 8–10). The use of the RAG-2-deficient blastocyst complementation system (11) allowed to bypass embryonic lethality and revealed that HIF-lα deficiency in *Rag-2*$^{-/-}$ chimeric mice results in

abnormal peritoneal B-1 cells, autoimmunity, and abnormal maturation of B-2 lymphocytes.

The striking cell-lineage specificity of the defects attributable to HIF-1α deficiency [no changes in T-cell subsets (Fig. 1) and distortion of B-1 and B-2 cell development] suggests that it is unlikely that these defects are because of nonspecific effects of HIF-1α deficiency on cell viability. Rather, they implicate HIF-1α in the control of B cell progenitor proliferation, which must occur by different mechanisms in B-1 and B-2 as compared with T cells based on our data. Indeed, proliferation of *Hif1*$\alpha^{-/-}$ B cells *in vivo* is inhibited in *Hif1*$\alpha^{-/-}$ mice (Fig. 5*D*). HIF-1α deficiency results in the depletion of highly proliferating cells among B cell progenitors in bone marrow, as CD43^{-} B220^{+} HSA^{high} cells, which are dramatically lost in *Hif1*$\alpha^{-/-} \rightarrow$ *Rag2*$^{-/-}$ chimeras (Fig. 5*B*), are the most highly proliferating subset. *Hif1*$\alpha^{-/-}$ CD43^{-}B220^{+} bone marrow cells also express much less Ki-67 when compared with CD43^{-}B220^{+} cells from *Hif1*$\alpha^{+/+}$ WT $\rightarrow$ *Rag2*$^{-/-}$ chimeras (Fig. 5*D*). These results indicate that HIF-1α deficiency may cause defects in proliferation of immature B cells and that the age-dependent distortion of B cell development in bone marrow may reflect the rate of B cell expansion.

The lymphoid phenotype of HIF-1α deficiency shares similarities and differences with other knockout mouse models (e.g., Btk, BSAP, and PI3K) (19–21), which were shown to play key roles in the development or homeostasis of B1 and B2 cells. Functional interactions between these gene products and HIF-1α may account for the overlapping phenotypes. For example, PI3K activity has been shown to control HIF-1α expression in prostate cancer cells (22).

The data presented here add to observations suggesting the importance of B-1 cells whose origin and functions have been the subject of controversy since they were first discovered (23). Thus, whereas the role of HIF-1 in mediating physiological responses to hypoxia is well established, these results demonstrate that HIF-1 also functions in a cell lineage-specific, cell-autonomous and differentiation stage-specific manner to regulate lymphocyte development and to control autoimmunity. Observations of autoimmunity point to the need for further investigations of the role of HIF-1α in controlling cell cycle as well as apoptosis in B-lymphocytes, as apoptosis is implicated in the elimination of autoreactive cells and HIF-1α was shown to regulate apoptosis-controlling molecules (7, 8), including p53 and NIP3. These data provide genetic evidence for the role of HIF-1α in the regulation of cell proliferation *in vivo* in any system and are in agreement with the implied role of HIF-1α as the switch to glycolysis in proliferating lymphocytes. These data are also consistent with the demonstration of a correlation between the expression of HIF-1α and Ki-67 in human cancers and trophoblast cells (24, 25). Recent observations of the role of glucose transporter-1 gene (GLUT-1) in lymphocyte homeostasis (24) further support the importance of HIF-1α, as GLUT-1 expression is controlled by HIF-1 (4, 7). Perhaps the most striking cell-surface abnormality revealed in the analysis of peritoneal B-1 cells was the marked elevation of B220 (CD45, a receptor-associated protein tyrosine phosphatase) (Fig. 2*B*), which is one of the critical modulators of B cell receptor signaling and B lymphocyte development and activation (25). The reported data suggest that HIF-1α expression in B-1 lymphocytes could be required for down-regulation of CD45 (B220) expression during normal B-1 cell development. Additional studies are necessary to delineate the exact molecular pathways by which HIF-1α deficiency results in CD45 overexpression in B-1 cells and the consequences of CD45 overexpression with respect to the pathogenesis of autoimmunity.

Taken together, these observations suggest the need to analyze the possibility of autoimmunity as being the outcome of metabolic defects in immune cells and point to the HIF-1α as a promising subject of autoimmunity studies. The future directions of research are also suggested by recent demonstration of selective up-regulation of the alternatively spliced HIF-1α mRNA isoform I.1, an immediate early response gene that encodes the HIF-1α protein without the first 12 N-terminal amino acids in activated lymphocytes (26). It remains to be established whether the effects of HIF-1α deficiency observed here are because of the requirements in this "short" I.1 isoform or in the I.2 isoform, which encodes the "classical" HIF-1α.

We thank Drs. W. E. Paul, R. N. Germain, K. Yasutomo, M. Murakami, S. Apasov, G. Gomez, and P. Smith (Laboratory of Immunology, National Institute of Allergy and Infectious Diseases, National Institutes of Health) for help and discussions. We thank Brenda Marshall and Shirley Starnes for help in preparation of the manuscript. This work was supported by a research grant from the Seki Minato Foundation (to H.K.), a grant from Welfide Medicinal Research Foundation (to H.K.), and a grant from Nagao Memorial Fund (to H.K.).

1. Picker, L. J. & Siegelman, M. H. (1999) *Fundamental Immunology* (Lippincott, Philadelphia).
2. Caldwell, C. C., Kojima, H., Lukashev, D., Armstrong, J., Farber, M., Apasov, S. & Sitkovsky, M. V. (2001) *J. Immunol.* **167,** 6140–6149.
3. Brand, K. A. & Hermfisse, U. (1997) *FASEB J.* **11,** 388–395.
4. Ratcliffe, P. J., O'Rourke, J. F., Maxwell, P. H. & Pugh, C. W. (1998) *J. Exp. Biol.* **201,** 1153–1162.
5. Iyer, N. V., Kotch, L. E., Agani, F., Leung, S. W., Laughner, E., Wenger, R. H., Gassmann, M., Gearhart, J. D., Lawler, A. M., Yu, A. Y. & Semenza, G. L. (1998) *Genes Dev.* **12,** 149–162.
6. Wang, G. L., Jiang, P. H., Rue, E. A. & Semenza, G. L. (1995) *Proc. Natl. Acad. Sci. USA* **92,** 5510–5514.
7. Semenza, G. L. (2000) *J. Appl. Physiol.* **88,** 1474–1480.
8. Carmeliet, P., Dor, Y., Herbert, J-M., Fukumuras, D., Brusselmans, K., Dewerchin, M., Neeman, M., Bono, F., Abramovitch, R., Maxwell, P., *et al.* (1998) *Nature (London)* **394,** 485–490.
9. Kotch, L. E., Iyer, N. V., Laughner, E. & Semenza, G. L. (1999) *Dev. Biol.* **209,** 254–267.
10. Ryan, H. E., Lo, J. & Johnson, R. S. (1998) *EMBO J.* **17,** 3005–3015.
11. Chen, J., Lansford, R., Stewart, V., Young, F. & Alt, F. W. (1993) *Proc. Natl. Acad. Sci. USA* **90,** 4528–4532.
12. Carmeliet. P., Ferreira, V., Breier, G., Pollefeyt, S., Kiechens, L., Gertsenstein, M., Fahrig, M., Vandenhoeck, A., Harpal, K., Eberhardt, C., *et al.* (1996) *Nature (London)* **380,** 435–439.
13. Rolink, A., Grawunder, U., Winkler, T. H., Karasuyama, H. & Melchers, F. (1994) *Int. Immunol.* **6,** 1257–1264.
14. Chen, J., Ma, A., Young, F. & Alt, M. (1994) *Int. Immunol.* **6,** 1265–1268.
15. Hayakawa, K., Hardy, R. R., Honda, M., Herzenberg, L. A., Steinberg, A. D. & Herzenberg, L. A. (1984) *Proc. Natl. Acad. Sci. USA* **81,** 2494–2498.
16. Theofilopoulos, A. N. & Dixon, F. J. (1985) *Adv. Immunol.* **37,** 269–390.
17. Hardy, R. R., Carmack, C. E., Shinton, S. A., Kemp, J. D. & Hayakawa, K. (1991) *J. Exp. Med.* **173,** 1213–1225.
18. Key, G., Becker, M. H., Baron, B., Duchrow, M., Schluter, C., Flad, D. & Gerdes, J. (1993) *Lab. Invest.* **68,** 629–636.
19. Fruman, D. A., Snapper, S. B., Yballe, C. M., Davidson, L., Yu, J. Y., Alt, F. W. & Cantley, L. C. (1999) *Science* **283,** 393–397.
20. Urbanek, P., Wang, Z. Q., Fetka, I., Wagner, E. F. & Busslinger, M. (1994) *Cell* **79,** 901–912.
21. Khan, W. N., Alt, F. W., Gerstein, R. M., Malynn, B. A., Larsson, I., Rathbun, G., Davidson, L., Muller, S., Kantor, A. B. & Herzenberg, L. A. (1995) *Immunity* **3,** 283–299.
22. Zhong, H., Chiles, K., Feldser, D., Laughner, E., Hanrahan, C., Georgescu, M. M., Simons, J. W. & Semenza, G. L. (2000) *Cancer Res.* **60,** 1541–1545.
23. Wortis, H. N. & Berland, R. (2001) *J. Immunol.* **166,** 2163–2166.
24. Rathmell, J. C., Vander Heiden, M. G., Harris, M. H., Frauwirth, K. A. & Thompson, C. B. (2000) *Mol. Cell* **6,** 683–692.
25. Trowbridge, I. S. & Thomas, M. L. (1994) *Annu. Rev. Immunol.* **12,** 85–116.
26. Lukashev, D. E., Caldwell, C. C., Ohta, A., Chen, P. & Sitkovsky, M. V. (2001) *J. Biol. Chem.* **276,** 48754–48763.